

# Iron Dyshomeostasis Induces Binding of APP to BACE1 for Amyloid Pathology, and Impairs APP/Fpn1 Complex in Microglia: Implication in Pathogenesis of Cerebral Microbleeds

Li Gong<sup>1,\*</sup>, Xiangzhu Tian<sup>1,\*</sup>, Jing Zhou<sup>2,\*</sup>, Qiong Dong<sup>1</sup>, Yan Tan<sup>1</sup>, You Lu<sup>1</sup>, Jiayan Wu<sup>1</sup>, Yanxin Zhao<sup>1</sup>, and Xueyuan Liu<sup>1</sup>

Cell Transplantation  
2019, Vol. 28(8) 1009–1017  
© The Author(s) 2019  
Article reuse guidelines:  
sagepub.com/journals-permissions  
DOI: 10.1177/0963689719831707  
journals.sagepub.com/home/ct  


## Abstract

As a putative marker of cerebral small vessel disease, cerebral microbleeds (CMBs) have been associated with vascular cognitive impairment. Both iron accumulation and amyloid protein precursor (APP) dysregulation are recognized as pathological hallmarks underlying the progression of CMBs, but their cross-talk is not yet understood. In this study, we found a profound increase of amyloid formation with increasing FeCl<sub>3</sub> treatment, and a distinct change in APP metabolism and expression of iron homeostasis proteins (ferritin, Fpn1, iron regulatory protein) was observed at the 300 μM concentration of FeCl<sub>3</sub>. Further results revealed that extracellular iron accumulation might potentially induce binding of APP to BACE1 for amyloid formation and decrease the capability of APP/Fpn1 in mediating iron export. Our findings in this study, reflecting a probable relationship between iron dyshomeostasis and amyloid pathology, may help shed light on the underlying pathogenesis of CMBs in vascular cognitive impairment.

## Keywords

cerebral microbleeds, small vessel disease, iron, amyloid protein precursor, ferritin

## Introduction

Cerebral microbleeds (CMBs), regarded as a putative marker of cerebral small vessel disease (cSVD), have been associated with cognitive decline in patients with stroke and vascular cognitive impairment. Histologically, CMBs may not only represent the extracellular accumulation of hemosiderin from leakage through cerebral small vessels and pathological iron deposition following hemorrhage and ferritin breakdown, but also correlate with cerebral amyloid angiopathy<sup>1-4</sup>. Furthermore, several observational studies support that CMBs may relate to amyloid deposition in dementia<sup>5-9</sup>, and the key finding revealed that ferritin, as a major iron storage protein, adversely impacts dementia progression<sup>10</sup>.

Previous evidence indicated a key mechanism of Aβ toxicity underlying dysregulated processing of amyloid protein precursor (APP) via the switch from the non-amyloidogenic to the amyloidogenic pathway. In the amyloidogenic pathway, APP is cleaved by β-secretase (BACE1) and γ-secretase, leading to increased Aβ<sub>42</sub> generation<sup>11,12</sup>. In the non-amyloidogenic pathway, the protective upregulation of APP

by the iron regulatory protein (IRP) can be linked to the finding that active interaction of APP with surface ferroportin1 (Fpn1) could not only mediate excessive iron efflux but also maintain cognitive function<sup>13-16</sup>. Since both the extracellular iron dyshomeostasis and amyloid deposition are recognized as pathological hallmarks of CMBs, insight into the relationship between them might not only increase understanding of the

<sup>1</sup> Department of Neurology, Shanghai Tenth People's Hospital, Tongji University, Shanghai, China

<sup>2</sup> Department of Neurosurgery, Binhai people's hospital, Jiangsu Province, China

\* Li Gong, Jing Zhou and Xiangzhu Tian contributed equally to this article

Submitted: July 11, 2018. Revised: December 22, 2018. Accepted: January 17, 2019.

## Corresponding Authors:

Xueyuan Liu and Yanxin Zhao, Department of Neurology, Shanghai Tenth People's Hospital, Tongji University, 301# Middle Yanchang Road, Shanghai 200072, China.

Emails: Liuxy@tongji.edu.cn; zhao\_yanxin@126.com



underlying pathogenesis of cSVD, but also convey their importance in vascular cognitive impairment.

Therefore, in the present study, we hypothesized APP as a key link between iron dysregulation and pathogenesis of CMBs, and analyzed the effects of extracellular iron treatment on APP metabolism and its association with the proteins of iron homeostasis including ferritin, Fpn1, and IRP. Considering that the APP/Fpn1 complex mediates iron export at the plasma membrane where APP combines with BACE1, we further investigated changes in the interaction of both complexes in response to iron treatments. Rather than storing a large content of iron, previous findings supported that microglia can rapidly de novo synthesize APP as an acute phase protein in response brain injury<sup>17,18</sup>; therefore, we used microglia as a model cell line, not neurons. Our findings support a potential relation of extracellular iron dyshomeostasis with APP metabolism, and reflect the underlying pathogenesis of CMBs in the process of vascular cognitive dementia.

## Materials and Methods

### Cell

BV-2 cells (a microglia cell line) were obtained from the Peking Union Medical College (Beijing, China). Cells were maintained in Dulbecco's Modified Eagle medium (DMEM; Gibco, Carlsbad, CA, USA) containing 10% fetal bovine serum (FBS; Gibco), 100 U/ml penicillin, and 100 µg/ml streptomycin in a 5% CO<sub>2</sub> incubator at 37°C.

### Iron Treatment

Cells were cultured for 48 h with variable concentrations of FeCl<sub>3</sub> (Sangon Biotech, China) from 25 µM to 400 µM prior to Western blot analysis. Iron was kept soluble using L-ascorbic acid in Tris-HCl (pH = 7.5).

### Western Blot

Cells were washed and lysed. Protein concentrations were determined using BCA protein assay kit (Bio-Rad, Hercules, CA, USA). Aliquots of cell lysates containing ~20 mg of protein were subjected to 10% SDS-PAGE and subsequently blotted onto a PVDF membrane (Bio-Rad). After blocking in PBST with 5% bovine serum albumin for 1 h at room temperature, membranes were incubated with primary antibodies (anti-ferritin: 1:1000; anti-amyloid precursor protein: 1:20000; anti-ferroportin1: 1:200) at 4°C overnight. β-actin served as an internal reference, and the relative expression of target proteins was calculated. The protein bands were scanned into a computer with an Odyssey scanner (Li-COR, Biosciences, Lincoln, NE, USA).

### Quantitative Real-Time PCR

Total RNA extraction and cDNA synthesis were performed using TRIZOL reagent (Invitrogen, Grand Island, NY, USA)

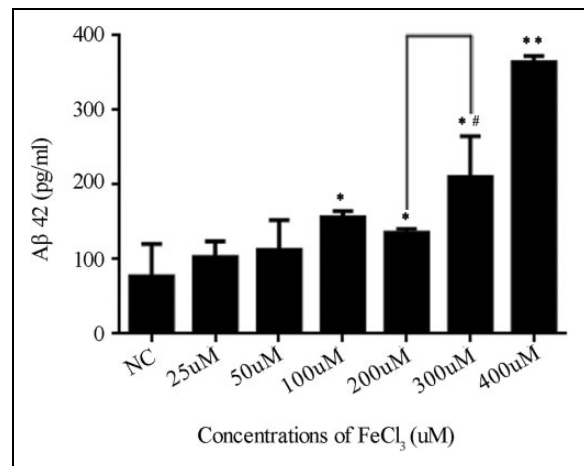


**Figure 1.** Effects of extracellular iron treatments on the changes in Aβ42 formation in microglia. Microglia was treated with increasing dose of FeCl<sub>3</sub> for 48 h after which the levels of Aβ42 were analyzed by ELISA. A significant increase in the level of Aβ42 ( $p < 0.01$ ) is observed at 300 µM FeCl<sub>3</sub> compared with that at 200 µM. Error bars represent mean  $\pm$  SEM ( $n = 3$ ). \* $p < 0.05$  and \*\* $p < 0.01$  as compared with control; # $p < 0.05$  as compared with 200 µM FeCl<sub>3</sub> treatment group.

and reverse transcription kit (TaKaRa, Tokyo, Japan) according to the manufacturers' instructions. The specific primers used for PCR are: APP forward, 5'-TTCTACACCAGGAGCGGAT-3', APP reverse, 5'-GGAAGTGTGCGATGCCACAGG-3'; ferritin forward, 5'-GCCCCTGAATCTGGCATGG-3', ferritin reverse, 5'-ATGCACTGCCTCAGTGACC-3'. Quantitative real-time PCR was performed using SYBR FAST qPCR Master Mix (KAPA) with appropriate TaqMan primers in ABI PRISM 7900HT Sequence Detection System (Kapa Biosystems, Wilmington, MA, USA). All mRNA expressions were normalized to that of β-actin as described previously<sup>19</sup>, and the detection was performed in triplicate.

### ELISA

Microglia were seeded onto 96-well plates. Cells were treated with different concentrations of FeCl<sub>3</sub> for another 48 h. Cell supernatants were collected, and the Aβ42 levels were determined by using an Aβ1-42 ELISA Kit (Roche Diagnostic GmbH, Mannheim, Germany).

### siRNA Transfection

Cells were transfected with non-targeting siRNA (negative control) or special siRNA targeting rat APP (5'-CUCAA-CAUGCACAUGAAUGdTdT-3') designed by Genepharma using Lipofectamine™2000 reagent (Invitrogen) according to the manufacturer's instructions. The medium was refreshed 6 h later, and cells were harvested 48 h later.

### Co-Immunoprecipitation (CoIP)

Cells were lysed in immunoprecipitation buffer (protease inhibitor and phosphatase inhibitor mixture). Equal

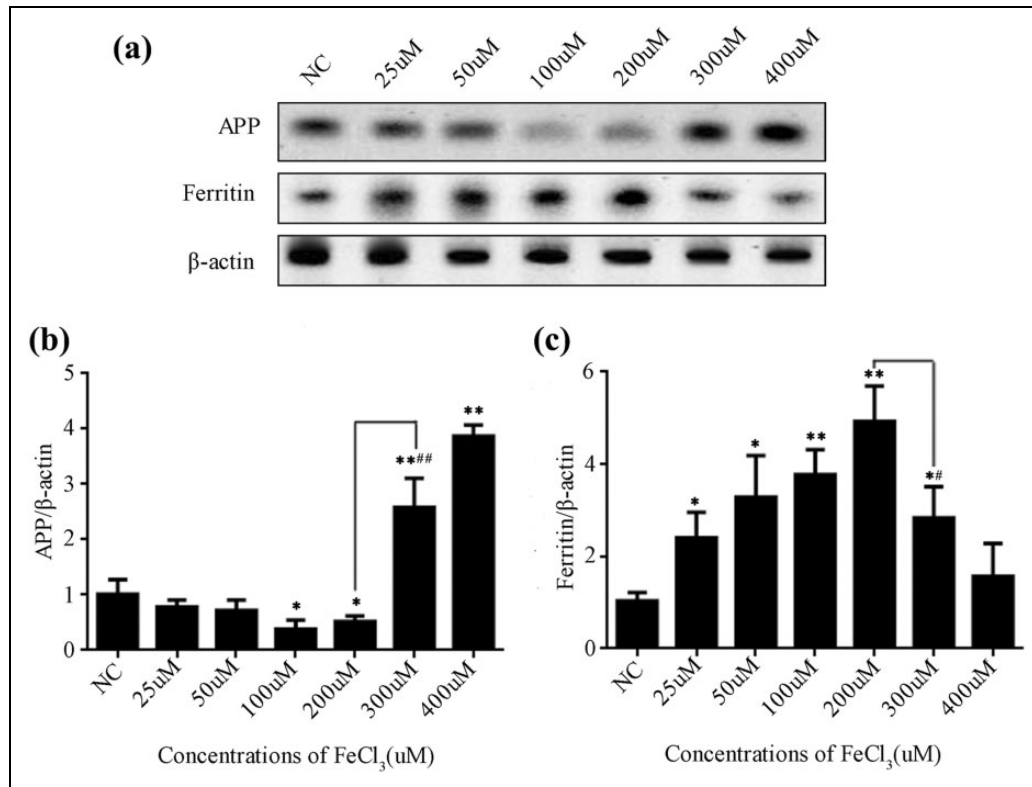


**Figure 2.** Effects of extracellular iron treatments on the levels of APP and ferritin proteins in microglia. Microglia was treated with increasing dose of  $\text{FeCl}_3$  for 48 h after which we evaluated the levels of APP and ferritin proteins by Western blot. Upper panel (a) shows representative blots and lower panels represent the relative quantification of band density in APP (b) and ferritin (c), respectively. Values represent mean  $\pm$  SEM ( $n = 4$ ). \* $p < 0.05$  and \*\* $p < 0.01$  as compared with control; # $p < 0.05$  and ## $p < 0.01$  as compared with 200  $\mu\text{M}$   $\text{FeCl}_3$  treatment group.

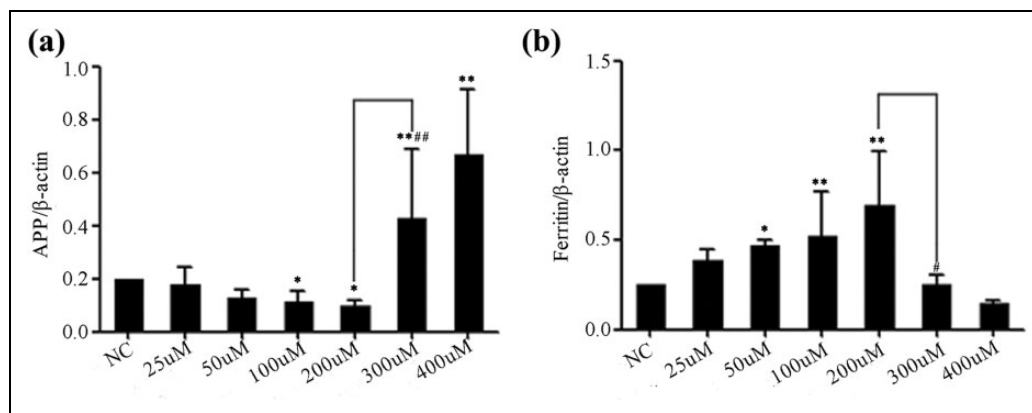


**Figure 3.** Effects of extracellular iron treatments on the changes in the mRNA levels of APP and ferritin in microglia. Microglia were treated with increasing doses of  $\text{FeCl}_3$  for 48 h. Relative mRNA expression levels of APP (a) and ferritin (b) were analyzed by RT-PCR. Values represent mean  $\pm$  SEM ( $n = 4$ ). \* $p < 0.05$  and \*\* $p < 0.01$  as compared with control; # $p < 0.05$  and ## $p < 0.01$  as compared with 200  $\mu\text{M}$   $\text{FeCl}_3$  treatment group.

amounts of protein (800  $\mu\text{g}$ ) from each sample were incubated with protein A/G agarose working solution for 10 min at  $4^\circ\text{C}$  under constant shaking. Then, 3  $\mu\text{g}$  of the specified antibody (APP: 1:30; ferroportin1: 1:50;

BACE1: 1:50) was added and incubated at  $4^\circ\text{C}$  overnight under constant shaking. After washing, the immune complexes in the supernatant were detected by Western blotting.

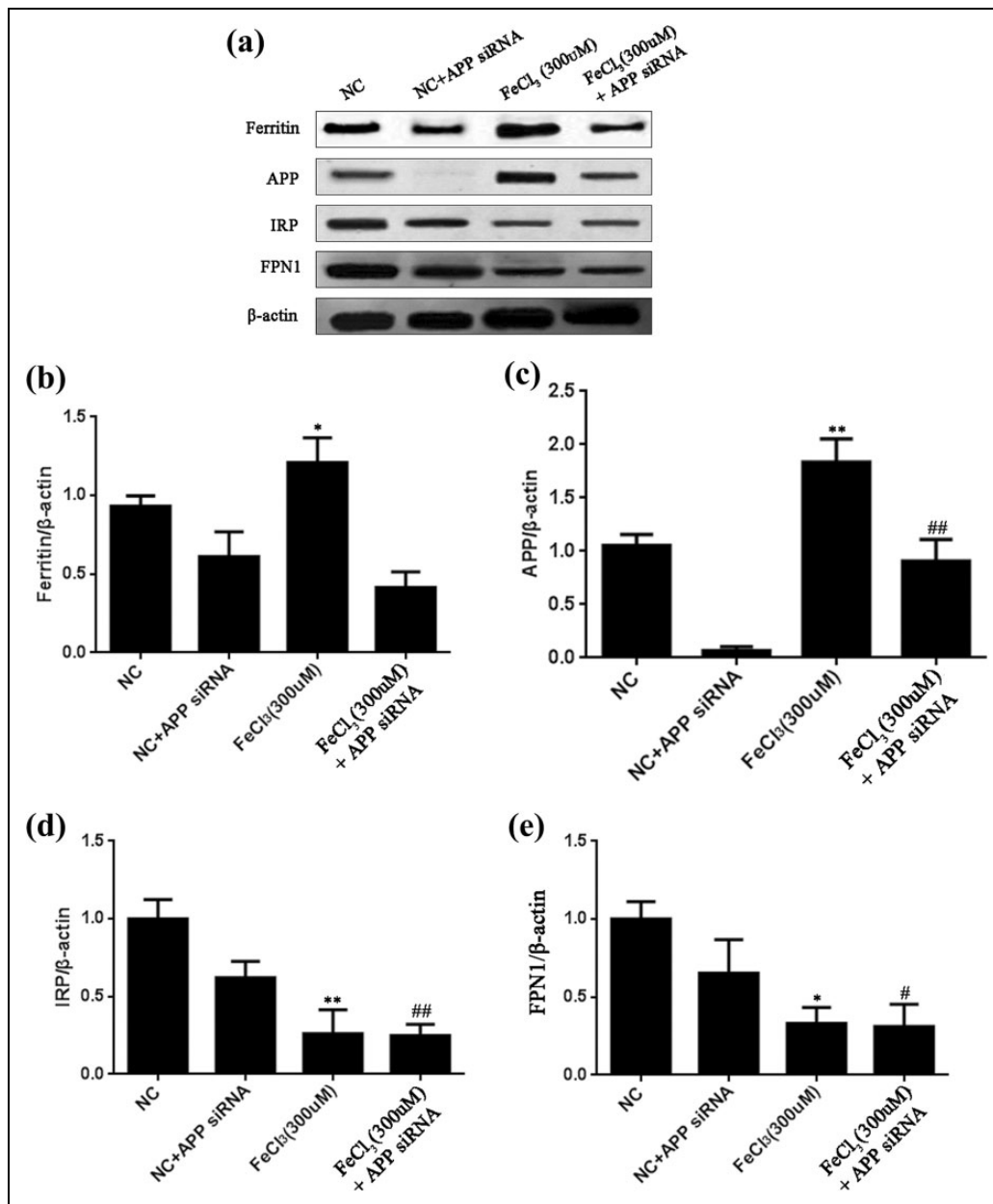


**Figure 4.** Extracellular iron treatments of microglia induce changes in the expression levels of iron metabolism proteins in the presence and absence of APP mediated by siRNA. Microglia was treated with 300  $\mu$ M iron treatment for 48 h. Changes in iron metabolism proteins were determined by Western blot. Panel (a) shows representative blots and the panels below show the quantification of band density in ferritin (b), APP (c), IRP (d), and Fpn I (e) in the presence and absence of APP, respectively. Values represent mean  $\pm$  SEM (n = 4). \*p < 0.05 and \*\*p < 0.01 as compared with control groups in the presence of APP; #p < 0.05 and ##p < 0.01 as compared with control groups in the absence of APP.

### Statistical Analysis

Data are presented as mean  $\pm$  SEM. Statistical analyses were completed using SPSS (SPSS Statistics v20; IBM, Armonk, NY, USA). All differences between the means were assessed by two-way analysis of variance (ANOVA), after which Bonferroni post hoc tests were conducted. P-values less than 0.05 were considered as statistically significant.

### Results

To ascertain whether iron treatment resulted in A $\beta$ 42 accumulation, we first evaluated the levels of A $\beta$ 42 by ELISA in microglia treated with increasing doses of FeCl<sub>3</sub>. Considering that brain iron is present at a concentration of approximately 1 mM surrounding amyloid plaques<sup>11</sup>, we controlled the iron concentration under this level. After 48 h treatments, we did not find cell viability CCK8 assay at 300  $\mu$ M

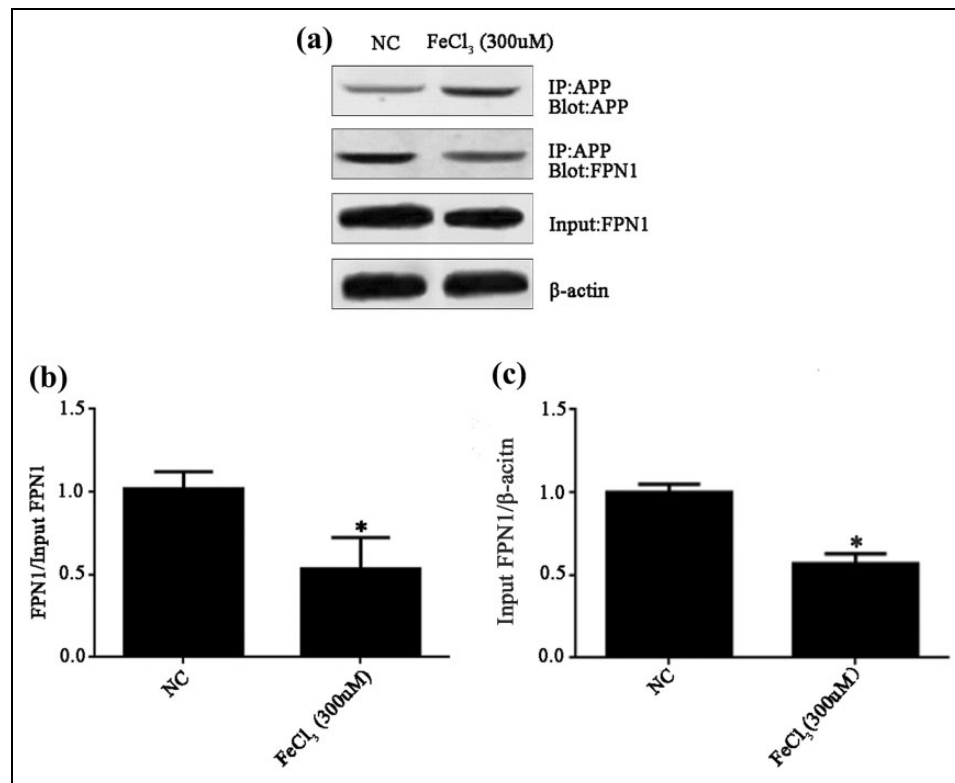


**Figure 5.** Extracellular iron treatments induce changes in the interaction of APP and FPN1 proteins in microglia. Microglia was treated with 300  $\mu$ M iron. Changes in the interaction of APP and FPN1 were analyzed by coimmunoprecipitation (CoIP). Panel (a) shows representative blots and lower panels show the ratio of band density in Blot:FPN1/Input:FPN1 (b), and quantification of band density in Input:FPN1 (c), respectively. Values represent mean  $\pm$  SEM ( $n = 3$ ). \* $p < 0.05$  as compared with control.

concentration of FeCl<sub>3</sub> reduced significantly as compared with control (Sup. 1). Next significantly increased levels of A $\beta$ 42 ( $p < 0.01$ ) were found at the concentration of 300  $\mu$ M (Fig. 1). We further characterized whether the increase in extracellular iron content was related to changes in the levels of iron transporters. Microglia treated with increasing FeCl<sub>3</sub> concentrations for 48 h showed reduced levels of APP proteins and elevated ferritin protein levels below 300  $\mu$ M treatment. When FeCl<sub>3</sub> concentrations reached 300  $\mu$ M, levels of APP protein in microglia significantly increased, while ferritin production was decreased (Fig. 2).

To determine if changes in microglial protein levels were consistent with changes in mRNA levels, qPCR was conducted after treatment with iron for 48 h using specific primers for APP and ferritin (Fig. 3). Results showed that changes in APP mRNA and ferritin mRNA were similar to the changes in their protein levels. Microglia treated with iron concentrations below 300  $\mu$ M presented decrease in APP mRNA content but increase in ferritin mRNA levels. APP mRNA increased significantly in microglia while decreased ferritin mRNA was observed following 300  $\mu$ M FeCl<sub>3</sub> treatment.

Considering that APP is suggested to be associated with amyloidogenesis and iron dyshomeostasis, it is of interest to determine the putative changes in iron metabolism proteins such as ferritin, IRP, and Fpn1 in the absence of APP. To this

end, we detected an increase in APP and ferritin proteins by 300  $\mu$ M iron treatment, and found decreased levels of IRP and Fpn1 proteins compared with control groups. In the absence of APP mediated by siRNA, iron treatment also induced a significant decrease in IRP and Fpn1 proteins and elevated APP proteins, whereas ferritin levels remained unchanged (Fig. 4).

According to the above changes, we next evaluated if microglia treated with iron could affect the interaction between APP and Fpn1 using a CoIP technique. Although CoIP results do not necessarily mean the interaction is direct, it suggests a probable binding capability of a complex. There was a reduced ratio of Blot: Fpn1/Input: Fpn1, likely due to a decreased affinity of APP/Fpn1, observed following iron treatment in treated groups compared with controls (Fig. 5). We also evaluated the change in binding of APP and BACE1 during the interaction APP/Fpn1, and found that iron treatment of microglia showed an increased interaction between APP/BACE1, without significant changes in the level of BACE1 (Fig. 6).

## Discussion

The pathological hallmarks of CMBs in the brain are not only increased extracellular iron deposition, but also

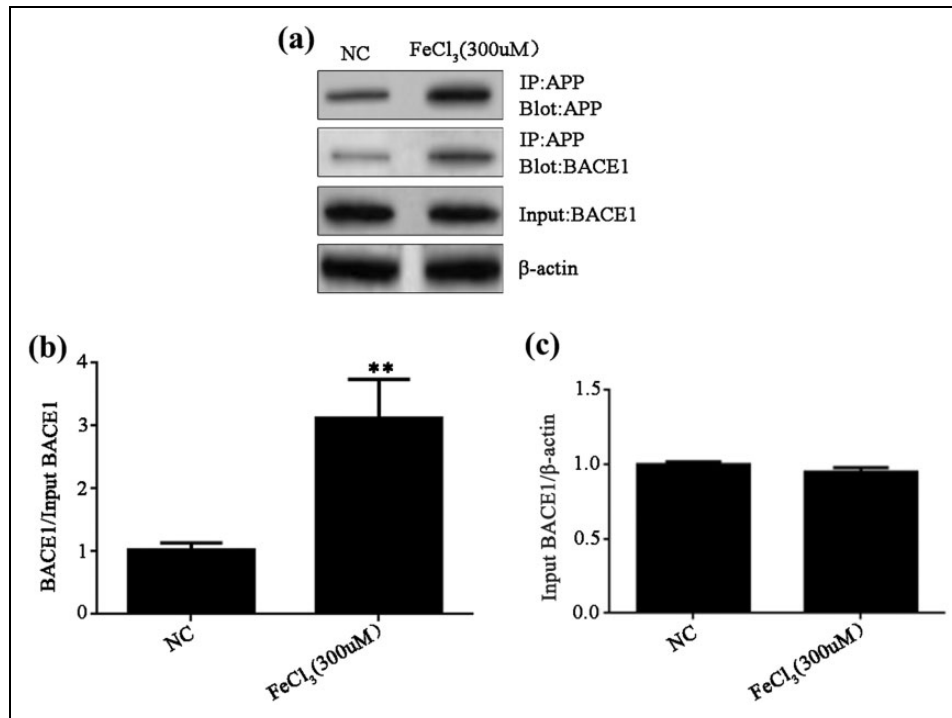


**Figure 6.** Extracellular iron treatments induce changes in the interaction of APP and BACE1 proteins in microglia. Microglia was treated with 300 μM iron. Changes in the interaction of APP and BACE1 were analyzed by CoIP. Panel (a) shows representative blots and lower panels show the ratio of band density in Blot:BACE1/Input:BACE1 (b), and quantification of band density in Input:BACE1 (c), respectively. Values represent mean  $\pm$  SEM ( $n = 3$ ). \*\* $p < 0.01$  as compared with control.

excessive amyloid plaques<sup>5</sup>. However, the molecular mechanisms of how amyloidosis and extracellular iron accumulation cross-talk remain unknown. Our results showed that extracellular iron treatment exercised profound effects on APP metabolism, and induced a significant increase of amyloid protein levels at the FeCl<sub>3</sub> concentration of 300 μM. Furthermore, a distinct change in APP metabolism and expression of iron homeostasis proteins (ferritin, Fpn1, IRP) was observed at the 300 μM concentration of FeCl<sub>3</sub>. We supposed that this concentration was likely to reflect the microglia status switching from the homeostasis to dysregulation in the present experimental condition. Finally, the increase in amyloid formation might be partially explained if extracellular iron accumulation was related to the reduced iron export by the complex of APP/Fpn1 and higher affinity of APP/BACE1. Our data provide a potential mechanism for the previous findings that CMBs are associated with amyloid pathology in the brain, the latter being related to the ferritin in CSF<sup>5,8,10</sup>.

In the central nervous system, the largest iron stores are found within microglia and modulated by ferritin, which plays the crucial role of controlling iron storage and homeostasis. Thus, microglia are supposed to be naturally responsible for the maintenance of the extracellular iron status among other brain cell types<sup>20</sup>. Moreover, rather than clearance of amyloid plaques, microglia can induce APP production as an acute phase protein in response to brain

attacks<sup>17,18</sup>. For these reasons, we used microglia as a model cell line in this study rather than neurons, which appeared to be commonly used in other experiments. In microglia, extracellular iron treatment at the concentration of 300 μM dramatically increased the levels of Aβ<sub>42</sub>. The rise in Aβ<sub>42</sub> by accumulated iron may be a consequence of the activation of oxidative stress (OS) signaling pathways resulting in excess amyloid production<sup>21-24</sup>. The cause for the slight increase in amyloid formation in response to iron treatment below 300 μM is unknown, but could be because of a compensatory response to reduce OS<sup>25,26</sup>.

Previous studies suggested that APP could serve as a cell-surface pro-inflammatory receptor on microglia, and that it regulates microglial activation<sup>27</sup>. To this end we assumed the transient decrease in APP could be a result of the neuroprotective response below iron concentrations of 300 μM. Likewise, the increase in ferritin could be the natural function of excess iron for storage in order to protect against the OS response by iron regulatory protein/iron responsive element (IRP/IRE) regulatory system<sup>28,29</sup>. However, microglia presented an inverse pattern, including significant increase in APP and reduction of ferritin, at iron concentrations of 300 μM and above. The levels of ferritin were reduced in the presence of iron treatment higher than 300 μM, probably as a consequence of ferritin degradation due to iron-dependent oxidation and reduced ferritin synthesis<sup>29</sup>. Increased APP in response to 300 μM iron treatment is consistent with the previous observation of IRP/APP IRE-

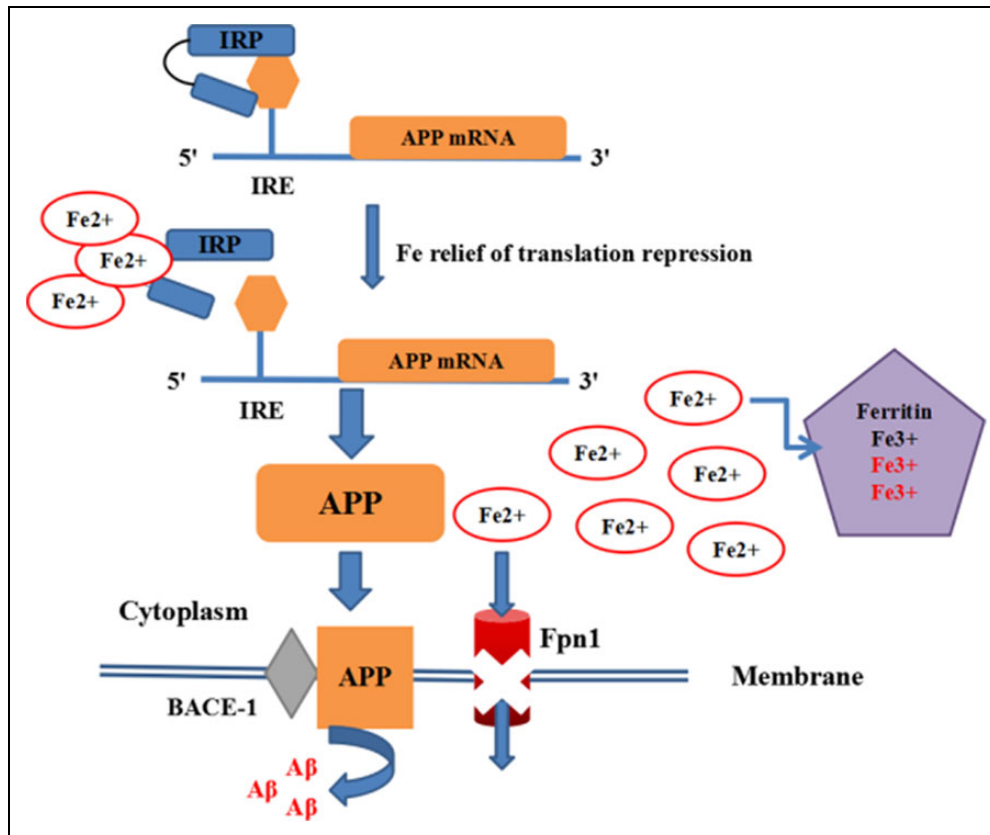


**Figure 7.** Schematic representation of changes in extracellular iron accumulation and amyloid formation in microglia. 300  $\mu$ M iron treatments of microglia elevated the APP protein level but reduced the levels of Fpn1 and IRP. Furthermore, the iron treatment might reduce the capability of APP/Fpn1 complex for iron efflux and induce binding of APP to BACE1 for amyloid protein production.

driven abundant iron efflux, and may be a response to severe oxidative challenges<sup>26</sup>.

To test the effects of APP on major iron metabolism proteins such as ferritin, IRP, and Fpn1 in microglia, we assessed the changes of these proteins in the absence of APP mediated by siRNA. Consistent with previous studies, down-regulated IRP levels following iron treatment could be a consequence of regulation of IRP/IRE iron homeostasis system<sup>11,15</sup>. Unexpectedly, it resulted in a significant reduction in Fpn1 protein, probably independent of the existence of APP. Although iron accumulation was thought to be associated with elevated Fpn1 levels, previous research showed that inflammatory stimuli caused by iron could decrease Fpn1 expression and trigger a positive feedback loop of elevated iron deposition in microglia<sup>30-32</sup>. It can be inferred that high iron concentrations may alter the expression of Fpn1 as we observed in this study.

Following the changes in the above proteins, such as the reduced level of Fpn1, it was of interest to evaluate if the affinity of interaction between increased APP and decreased Fpn1 could be affected. We used CoIP to show that there was a decreased level of Fpn1 immunoprecipitated by APP antibody, partially suggesting reduced affinity of the APP/Fpn1 complex. However, rather than the potential decreased

ability of interaction, this finding might be also attributed to the possibility of decreased input of Fpn1 protein amount itself. In addition, we also investigated whether the “relative excess” APP could turn to interact with BACE1, another membrane protein in microglia, during the binding of the APP/Fpn1 complex. The cause for the observed increase in the interaction of APP/BACE1 complex without significant changes in the level of BACE1 is unknown, but the process of interaction is a key step in the amyloid pathway. Therefore, it could partially explain why there is a significant increase in A $\beta$ 42 levels at iron concentrations of 300  $\mu$ M. Our findings might suggest a potential relationship for both complexes of APP/Fpn1 and APP/BACE1, providing new insights for further investigation; however, it should be carefully considered that CoIP does not mean the interaction is direct, since larger complexes may be involved.

In summary, extracellular iron accumulation induced a significant increase in amyloid formation, and was likely due to both the APP dysregulation and iron perturbation. Changes in extracellular iron accumulation might potentially induce the interaction between APP and BACE1 which is necessary for amyloid production, but also reduce the capability of APP/Fpn1 mediating iron homeostasis (Fig. 7). The data presented here establish a potential key link of

extracellular iron dyshomeostasis and APP metabolism, supporting the role of CMBs in the pathogenesis of vascular cognitive dementia.

### Ethical Approval

This study was approved by the Ethics Committee of Shanghai Tenth People's Hospital (Shanghai, China).

### Statement of Human and Animal Rights

This article does not contain any studies with human or animal subjects.

### Statement of Informed Consent

There are no human subjects in this article and informed consent is not applicable.

### Declaration of Conflicting Interests

The author(s) declared no potential conflicts of interest with respect to the research, authorship, and/or publication of this article.

### Funding

The author(s) disclosed receipt of the following financial support for the research, authorship, and/or publication of this article: This work was supported by grant from National Natural Science Foundation of China (No.81771131, No.81571033), and by Science and Technology Commission of Shanghai Municipality (No.17411950100, No.17411967500).

### ORCID iD

Li Gong  <https://orcid.org/0000-0002-8583-5108>

### Supplemental Material

Supplemental material for this article is available online.

### References

- Fazekas F, Kleinert R, Roob G, Kleinert G, Kapeller P, Schmidt R, Hartung HP. Histopathologic analysis of foci of signal loss on gradient-echo T2\*-weighted MR images in patients with spontaneous intracerebral hemorrhage: evidence of microangiopathy-related microbleeds. *AJNR Am J Neuroradiol.* 1999;20(4):637–642.
- Schrag M, McAuley G, Pomakian J, Jiffry A, Tung S, Mueller C, Vinters HV, Haacke EM, Holshouser B, Kido D, Kirsch WM. Correlation of hypointensities in susceptibility-weighted images to tissue histology in dementia patients with cerebral amyloid angiopathy: a postmortem MRI study. *Acta Neuropathol.* 2010;119(3):291–302.
- Liu Y, Liu J, Liu H, Liao Y, Cao L, Ye B, Wang W. Investigation of cerebral iron deposition in aged patients with ischemic cerebrovascular disease using susceptibility-weighted imaging. *Ther Clin Risk Manag.* 2016;12:1239–1247.
- Ping S, Qiu X, Gonzalez-Toledo ME, Liu X, Zhao LR. Stem cell factor in combination with granulocyte colony-stimulating factor reduces cerebral capillary thrombosis in a mouse model of CADASIL. *Cell Transplant.* 2018;27(4):637–647.
- Goos JD, Kester MI, Barkhof F, Klein M, Blankenstein MA, Scheltens P, van der Flier WM. Patients with Alzheimer disease with multiple microbleeds: relation with cerebrospinal fluid biomarkers and cognition. *Stroke.* 2009;40(11):3455–3460.
- Kester MI, van der Flier WM, Mandic G, Blankenstein MA, Scheltens P, Muller M. Joint effect of hypertension and APOE genotype on CSF biomarkers for Alzheimer's disease. *J Alzheimers Dis.* 2010;20(4):1083–1090.
- Cordonnier C, van der Flier WM. Brain microbleeds and Alzheimer's disease: innocent observation or key player? *Brain.* 2011;134(Pt 2):335–344.
- Kester MI, Goos JD, Teunissen CE, Benedictus MR, Bouwman FH, Wattjes MP, Barkhof F, Scheltens P, van der Flier WM. Associations between cerebral small-vessel disease and Alzheimer disease pathology as measured by cerebrospinal fluid biomarkers. *JAMA Neurol.* 2014;71(7):855–862.
- Shams S, Granberg T, Martola J, Li X, Shams M, Fereshtehnejad SM, Cavallin L, Aspelin P, Kristoffersen-Wiberg M, Wahlund LO. Cerebrospinal fluid profiles with increasing number of cerebral microbleeds in a continuum of cognitive impairment. *J Cereb Blood Flow Metab.* 2016;36(3):621–628.
- Ayton S, Faux NG, Bush AI. Alzheimer's disease neuroimaging initiative. Ferritin levels in the cerebrospinal fluid predict Alzheimer's disease outcomes and are regulated by APOE. *Nat Commun.* 2015;6:6760.
- Bandyopadhyay S, Rogers JT. Alzheimer's disease therapeutics targeted to the control of amyloid precursor protein translation: maintenance of brain iron homeostasis. *Biochem Pharmacol.* 2014;88(4):486–494.
- Ehrhart J, Darlington D, Kuzmin-Nichols N, Sanberg CD, Sawmiller DR, Sanberg PR, Tan J. Biodistribution of infused human umbilical cord blood cells in Alzheimer's disease-like murine model. *Cell Transplant.* 2016;25(1):195–199.
- Fujioka M, Taoka T, Matsuo Y, Mishima K, Ogoshi K, Kondo Y. Magnetic resonance imaging shows delayed ischemic striatal neurodegeneration. *Ann Neurol.* 2003;54(6):732–747.
- Rogers JT, Venkataramani V, Washburn C, Liu Y, Tummala V, Jiang H, Smith A, Cahill CM. A role for amyloid precursor protein translation to restore iron homeostasis and ameliorate lead (Pb) neurotoxicity. *J Neurochem.* 2016;138(3):479–494.
- Duce JA, Tsatsanis A, Cater MA, James SA, Robb E, Wikke K, Leong SL, Perez K, Johanssen T, Greenough MA, Cho HH, Galatis D, Moir RD, Masters CL, McLean C, Tanzi RE, Cappai R, Barnham KJ, Ciccotosto GD, Rogers JT, Bush AI. Iron-export ferroxidase activity of  $\beta$ -amyloid precursor protein is inhibited by zinc in Alzheimer's disease. *Cell.* 2010;142(6):857–867.
- Lei P, Ayton S, Finkelstein DI, Spoerri L, Ciccotosto GD, Wright DK, Wong BX, Adlard PA, Cherny RA, Lam LQ, Roberts BR, Volitakis I, Egan GF, McLean CA, Cappai R, Duce JA, Bush AI. Tau deficiency induces parkinsonism with dementia by impairing APP-mediated iron export. *Nat Med.* 2012;18(2):291–295.
- Banati RB, Gehrman J, Lannes-Vieira J, Wekerle H, Kreutzberg GW. Inflammatory reaction in experimental autoimmune encephalomyelitis (EAE) is accompanied by a microglial



- expression of the beta A4-amyloid precursor protein (APP). *Glia*. 1995;14(3):209–215.
18. Banati RB, Gehrmann J, Czech C, Mönning U, Jones LL, König G, Beyreuther K, Kreutzberg GW. Early and rapid de novo synthesis of Alzheimer beta A4-amyloid precursor protein (APP) in activated microglia. *Glia*. 1993;9(3):199–210.
  19. Moisan A, Favre I, Rome C, De Fraipont F, Grillon E, Coquery N, Mathieu H, Mayan V, Naegele B, Hommel M, Richard MJ, Barbier EL, Remy C, Detante O. Intravenous injection of clinical grade human MSCs after experimental stroke: functional benefit and microvascular effect. *Cell Transplant*. 2016;25(12):2157–2171.
  20. Lopes KO, Sparks DL, Streit WJ. Microglial dystrophy in the aged and Alzheimer's disease brain is associated with ferritin immunoreactivity. *Glia*. 2008;56(10):1048–1060.
  21. Honda K, Casadesus G, Petersen RB, Perry G, Smith MA. Oxidative stress and redox-active iron in Alzheimer's disease. *Ann N Y Acad Sci*. 2004;1012:179–182.
  22. Casadesus G, Smith MA, Zhu X, Aliev G, Cash AD, Honda K, Petersen RB, Perry G. Alzheimer disease: evidence for a central pathogenic role of iron-mediated reactive oxygen species. *J Alzheimers Dis*. 2004;6(2):165–169.
  23. Moreira PI, Siedlak SL, Aliev G, Zhu X, Cash AD, Smith MA, Perry G. Oxidative stress mechanisms and potential therapeutics in Alzheimer disease. *J Neural Transm*. 2005;112(7):921–932.
  24. Chang YH, Wu KC, Harn HJ, Lin SZ, Ding DC. Exosomes and stem cells in degenerative disease diagnosis and therapy. *Cell Transplant*. 2018;27(3):349–363.
  25. Avramovich-Tirosh Y, Amit T, Bar-Am O, Weinreb O, Youdim MB. Physiological and pathological aspects of A $\beta$  in iron homeostasis via 5'UTR in the APP mRNA and the therapeutic use of iron-chelators. *BMC Neurosci*. 2008;9(Suppl 2):S2.
  26. Cho HH, Cahill CM, Vanderburg CR, Scherzer CR, Wang B, Huang X, Rogers JT. Selective translational control of the Alzheimer amyloid precursor protein transcript by iron regulatory protein-1. *J Biol Chem*. 2010;285(41):31217–31232.
  27. Manocha GD, Floden AM, Rausch K, Kulas JA, McGregor BA, Rojanathammanee L, Puig KR, Puig KL, Karki S, Nichols MR, Darland DC, Porter JE, Combs CK. APP regulates microglial phenotype in a mouse model of Alzheimer's disease. *J Neurosci*. 2016;36(32):8471–8486.
  28. Mehlhase J, Sandig G, Pantopoulos K, Grune T. Oxidation-induced ferritin turnover in microglial cells: role of proteasome. *Free Radical Biol Med*. 2005;38(2):276–285.
  29. Mehlhase J, Gieche J, Widmer R, Grune T. Ferritin levels in microglia depend upon activation: modulation by reactive oxygen species. *Biochim Biophys Acta*. 2006;1763(8):854–859.
  30. Rathore KI, Redensek A, David S. Iron homeostasis in astrocytes and microglia is differentially regulated by TNF- $\alpha$  and TGF- $\beta$ 1. *Glia*. 2012;60(5):738–750.
  31. Urrutia P, Aguirre P, Esparza A, Tapia V, Mena NP, Arredondo M, González-Billault C, Núñez MT. Inflammation alters the expression of DMT1, Fpn1 and hepcidin, and it causes iron accumulation in central nervous system cells. *J Neurochem*. 2013;126(4):541–549.
  32. Li Y, Pan K, Chen L Ning JL, Li X, Yang T, Terrando N, Gu J, Tao GJ. Deferoxamine regulates neuroinflammation and iron homeostasis in a mouse model of postoperative cognitive dysfunction. *J Neuroinflammation*. 2016;13(1):268.